doi:10.3788/gzxb20184710.1011002

基于二元互补调制模式的波前重构

庞博清[1,2,3],王帅[1,3],杨平[1,3]
(1 中国科学院自适应光学重点实验室,成都 610209)
(2 中国科学院大学,北京 100049)
(3 中国科学院光电技术研究所,成都 610209)

摘 要:为了提高波前探测过程中的波前采样频率,提出了一种基于二元互补模式的波前重构方法.该方法利用二元互补调制模式下获得的远场焦点光强信息对光场实部进行重构,进而通过光束的光强分布对光场虚部进行重构.该方法避免了额外调制模式的使用,将波前重构过程中所使用的调制模式的数量缩减为原有方法的 2/3,提升了波前采样频率.通过数值仿真对光强分布不均匀的待测光束的波前进行了重构,并利用实验对倾斜像差进行了测量重构,验证了该方法的可行性.

关键词:自适应光学;波前探测;振幅调制;波前像差;大气湍流;Zernike 拟合
中图分类号:O436 **文献标识码**:A **文章编号**:1004-4213(2018)10-1011002-10

Wavefront Reconstruction Based on Binary Complementary Modulation Modes

PANG Bo-qing[1,2,3], WANG Shuai[1,3], YANG Ping[1,3]
(1 *Key Laboratory on Adaptive Optics, Chinese Academy of Sciences, Chengdu* 610209, *China*)
(2 *University of Chinese Academy of Sciences, Beijing* 100049, *China*)
(3 *Institute of Optics and Electronics, Chinese Academy of Sciences, Chengdu* 610209, *China*)

Abstract: In order to improve the wavefront sampling frequency in wavefront detection, a wavefront reconstruction method based on two element complementary mode is proposed. The method reconstructs the real part of the light field by using the far field focal light intensity obtained under binary complementary modulation mode, and then reconstructs the imaginary part of the light field through the light intensity distribution of the beam. The method avoids the use of additional modulation mode, which reduces the number of modulation modes used in the process of wavefront sampling to 2/3 of the original method, and improves the wavefront sampling frequency. The wavefront of the beam with uneven intensity distribution is reconstructed in the numerical simulation, and the tilt aberration is reconstructed by experiments, which verify the feasibility of the method.

Key words: Adaptive optics; Wavefront sensing; Amplitude modulation; Wavefront aberration; Atmospheric turbulence; Zernike fitting
OCIS Codes: 110.1080; 010.7350; 010.1080; 120.5050; 120.5060; 110.6770

0 Introduction

Wavefront sensing plays an indispensable role inmodern optics. It is widely used in optical testing, ophthalmology and adaptive optics. Presently, most of the available wavefront sensing techniques include the Shack-Hartmann sensor [1-3], curvature sensing [4-6] and phase retrieval [7-9]. These wavefront sensing methods acquire the wavefront by analyzing the intensity distribution detected with array detectors. The

Foundation item: The National Fund of Chinese Academy of Sciences (No. CXJJ-16M208), the National Key Scientific Equipment Development Project of China (No.ZDYZ2013-2), Outstanding Youth Fund of Sichuan Province (No.2012JQ0012).
First author: PANG Bo-qing (1990—), male, Ph. D degree candidate, mainly focuses on wavefront sensing. Email: pangboqing@126.com
Supervisor (Contact author): YANG Ping (1980—), male, professor, Ph. D. degree, mainly focuses on adaptive optics. Email: pingyang2516@163.com
Received: Mar.20, 2018; **Accepted**: Jul.5, 2018

array detectors also have significant limitations in speed. It restricts the step of applying these techniques to detecting the wavefront which is stochastic and vary rapidly. Meanwhile, a large amount of data is produced in measurement. The transmission and operation of the mass data also consume a lot of time.

However, the wavefront sensing method based on single detector can deal with it well. Single detectors usually have mature manufacturing process and outstanding performance in practice. It can works well at high speed. Meanwhile, full aperture light is focused in the wavefront sensing method. So the focus light intensity contains the wavefront information of the whole aperture. More effective measurement information can be acquired in the method. Basing on the study results in existence, as few as dozens of signals can realize the wavefront reconstruction[10-11]. In order to explore the wavefront sensing method, a great deal of research has been done[10-14]. The wavefront sensing method through measurements of binary aberration modes is one of the valuable directions. It realizes wavefront sensing by acquiring the expansion coefficients of the aberration modes directly. Based on spatial light phase or intensity modulation, many researches have shown its great worth[10-11]. But, the traditional iterative algorithm and optimization strategy cannot reconstruct wavefront accurately and quickly. Non-uniqueness and slow convergence limits its use. Although the method realizing wavefront reconstruction by adding extra modulation patterns can realize wavefront reconstruction quickly and precisely, the added extra patterns mean that extra time is consumed[14].

Here, a wavefrontrconstruction method is introduced based on binary complementary modulation modes. In the method, complementary modulation modes are used to modulate the incident light and the focus light intensities are acquired to reconstruct the real part of the optical field. Then the intensity distribution of the incident light is introduced to determine the imaginary part, which reduces the number of the modulation functions used in the modulation. The incident wavefront is reconstructed quickly and precisely while the number of the modulation functions is reduced. The feasibility of the method is validated with numerical simulation and experiment.

1 Principle of wavefront sensing

The optical arrangement of the wavefront sensor is shown in Fig.1. In this schematic arrangement, the incident light is modulated with Digital Micromirror Device (DMD) firstly. Then the modulated light beam is focused with focus into the pinhole. The Photodiode (PD) is used to detect the light intensity of the focal point.

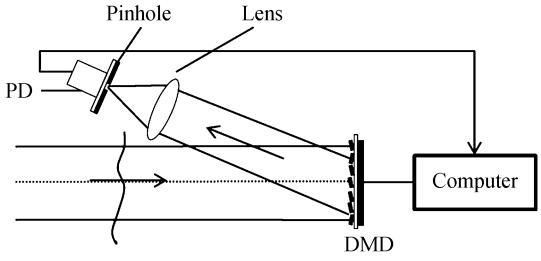

Fig.1 Schematic setup for the proposed wavefront sensing method

In the optical arrangement, DMD works as the spatial light modulator. It consists of an array of moving micromirrors, as shown in Fig. 2[15].

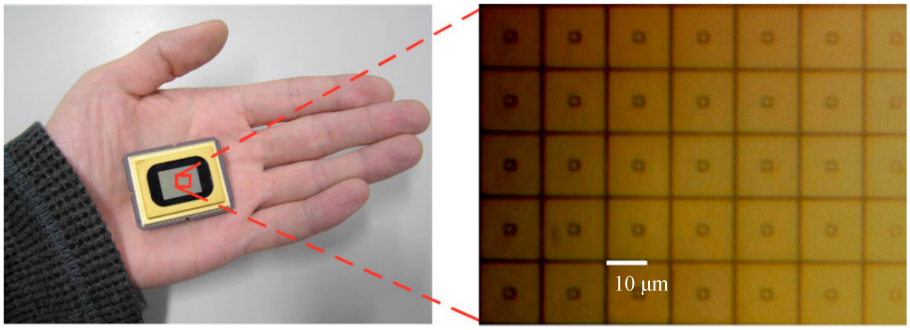

Fig.2 The micromirror array of DMD

Each micromirror can be rotated to either a $+12°$ or $-12°$ positions along the diagonal direction. It acts as an on/off switch and produces two modulation state, light on and light off. So the modulation functions can be expressed with these functions which have two values, 0 and 1. The Walsh functions are a series of binary and orthogonal functions [16-17]. They also have only two values, -1 and 1. So they can express modulation functions by simple line transformation. In order to express the modulation functions of the optical field over a circular aperture, the two-dimensional Walsh series for the polar coordinate are necessary. They are generated by the segments formed by dividing the azimuth angle and the radius over the circular aperture[10]. Fig. 3 shows the Walsh functions with the circular divided into 16 segments[14].

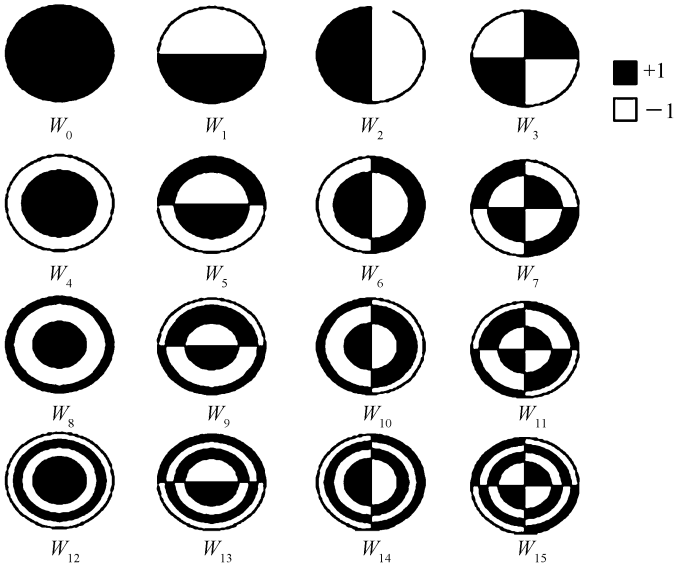

Fig.3 The Walsh functions for the polar coordinate when the circular aperture is divided into 16 segments

According to the Fourier diffraction theory, the amount of light in the ideal focal point collected from an incoming optical field $E(x, y)$ can be given by [12]

$$I = D_0 \cdot \left| \iint_A E(x,y)\,\mathrm{d}x\,\mathrm{d}y \right|^2 = D_0 \cdot \left| \iint_A A\,\mathrm{e}^{\mathrm{i}\varphi}\,\mathrm{d}x\,\mathrm{d}y \right|^2 \tag{1}$$

where A and φ are the amplitude and phase of the incident light, D_0 is a constant. The incident optical field is expanded with the Walsh series as follows

$$E(x,y) = A\,\mathrm{e}^{\mathrm{i}\varphi} = A\cos\varphi + \mathrm{i}\cdot A\sin\varphi = \sum_{l=0}^{N} a_l W_l + \mathrm{i}\cdot \sum_{l=0}^{N} b_l W_l = \sum_{l=0}^{N} B_l W_l \tag{2}$$

where index l can be any integer from 0 to N, W_l is the lth Walsh function, a_l and b_l are the lth Walsh function expansion coefficients of the real part and the imaginary part of the optical field, and

$$B_l = a_l + \mathrm{i}\cdot b_l \tag{3}$$

Thecomplementary modulation functions are generated to modulate the incident optical field, as follows

$$\begin{cases} T_k = \dfrac{1+W_k}{2} \\ T_k' = 1 - T_k = \dfrac{1-W_k}{2} \end{cases} \tag{4}$$

where the index k can be any integer from 0 to N, W_k is the kth Walsh function. T_k and T_k' are the complementary modulation patterns produced based on W_k. As discussed in Ref.[14], modulating the incident light with the modulation functions shown in Eq. (4), the light intensities collected with PD can be written as

$$\begin{cases} I_k = \dfrac{D_0}{4} \cdot |B_0 + B_k|^2 \\ I_k' = \dfrac{D_0}{4} \cdot |B_0 - B_k|^2 \end{cases} \tag{5}$$

And the expansion coefficients of the real part and the imaginary part of the optical field can be written as

$$\begin{cases} a_0=\sqrt{\dfrac{I_0}{D_0}},b_0=0 & k=0 \\ a_k=\dfrac{(I_k-I_k')}{\sqrt{I_0D_0}},|b_k|=\sqrt{\dfrac{2((I_k+I_k'))}{D_0}-a_0^2-a_k^2} & k\geqslant 1 \end{cases} \tag{6}$$

By now, the coefficients of the real part of the optical field is determined and the real part can be reconstructed by

$$A\cos\varphi=\sqrt{D_0}\cdot\sum_{l=0}^{N}a_lW_l \tag{7}$$

where $\sqrt{D_0}$ is unknown. As above discussed, the coefficient of the imaginary part of the optical field, b_0, is zero. When $l\geqslant 1$, the mean of W_l is zero. It means the average value of the imaginary part is zero. Considering that the optical field is continuous, there is a point whose imaginary part value equal to zero or approximately zero in the optical field. The absolute value of $\cos\varphi$ is 1. So the value of D_0 can be acquired based on

$$D_0=[\max(\left|\sum_{l=0}^{N}a_lW_l/A\right|)]^2 \tag{8}$$

Moduli of both sides of Eq.(2) equal to each other, which can be described with

$$A^2=D_0[(\sum_{l=0}^{N}b_lW_l)^2+(\sum_{l=0}^{N}a_lW_l)^2] \tag{9}$$

where A^2 is the light intensity distribution of the incident light. The Eq.(9) establishes a relationship among the light intensity distribution and the coefficients of the real and imaginary part of the optical field. It can be regarded as the quadric multiple equation and b_l is unknown variable of the Eq.(9). And considering l can be very large, it would be hard to solve Eq. (9) directly.

Considering that only the sign of b_l is unknown and the absolute value of b_l is determined in Eq. (9). For different sign of b_l, different optical field can be acquired. But only when all the sign of b_l is right, could Eq. (9) be tenable. So the determination of the sign of b_l can be transformed into the solution to the minimization of

$$\hat{d}=\left\|\frac{A^2}{D_0}-(\sum_{l=0}^{N}b_lW_l)^2-(\sum_{l=0}^{N}a_lW_l)^2\right\|_2 \tag{10}$$

The solution of Eq. (10) is different with the traditional common optimization. The only uncertainty in Eq. (10) is the signs of b_l. So the sign of b_l can be determined quickly. The minimization of $\hat{d}$ can be gotten just by changing the signs of b_l. Meanwhile, the sign of b_l is determined. Then the imaginary part of the optical can be described as

$$A\sin\varphi=\sqrt{D_0}\sum_{l=0}^{N}b_lW_l \tag{11}$$

By now, the optical field is reconstructed.The wavefront can be expressed as

$$\varphi=\mathrm{i}^{-1}\ln(\sum_{l=0}^{N}B_lW_l/A) \tag{12}$$

The wavefront acquired by Eq.(12) is wrapped and its range is $[-\pi,\pi]$. So phase unwrapping is required for reconstructing the wavefront. Based on the Nyquist sampling theory, we can reconstruct a discrete wavefront which is similar to the incident wavefront when the phase difference of the neighboring segments of φ is less than π [18]. A fluent wavefront can be determined by transforming the discrete wavefront into a smoothing wavefront expressed with the Zernike polynomials [19].

In the wavefront reconstruction method, the wavefront reconstruction procedure is as follows: 1) The calculation of the focal intensities. The complementary modulation functions, T_k and T_k', generated based on Walsh functions, W_k, are used to modulate the incident light. And the focal intensities, I_k and I_k', are calculated. 2) The real part reconstruction. The coefficients of the real part and the absolute value of the coefficients of the imaginary part can be determined by the focal intensities. The real part can be reconstructed with the coefficients of the real part. 3) The imaginary part reconstruction. A constraint on

the imaginary part is built based on the relationship between the light intensity distribution and the imaginary part. Then an equation is built to determine the sign of the coefficients of the imaginary. The imaginary part can be reconstructed with the coefficients. 4) Wavefront reconstruction. A discrete and wrapped wavefront can be acquired from the reconstructed optical field. Then an accurate reconstruction wavefront can be acquired by phase unwrapping and smoothing.

2 Numerical simulation

An incident wavefront is produced withthe first 35 Zernike polynomials depending on the power spectrum of the Kolmogorov model for atmospheric turbulence[20]. Fig. 4 shows the synthesized incident wavefront. Fig. 4(a) is the incident wavefront and Fig. 4(b) is the amplitude of the optical field and the value of the amplitude is 1. Fig. 4(c) and Fig. 4(d) are the real part and the imaginary part of the optical field.

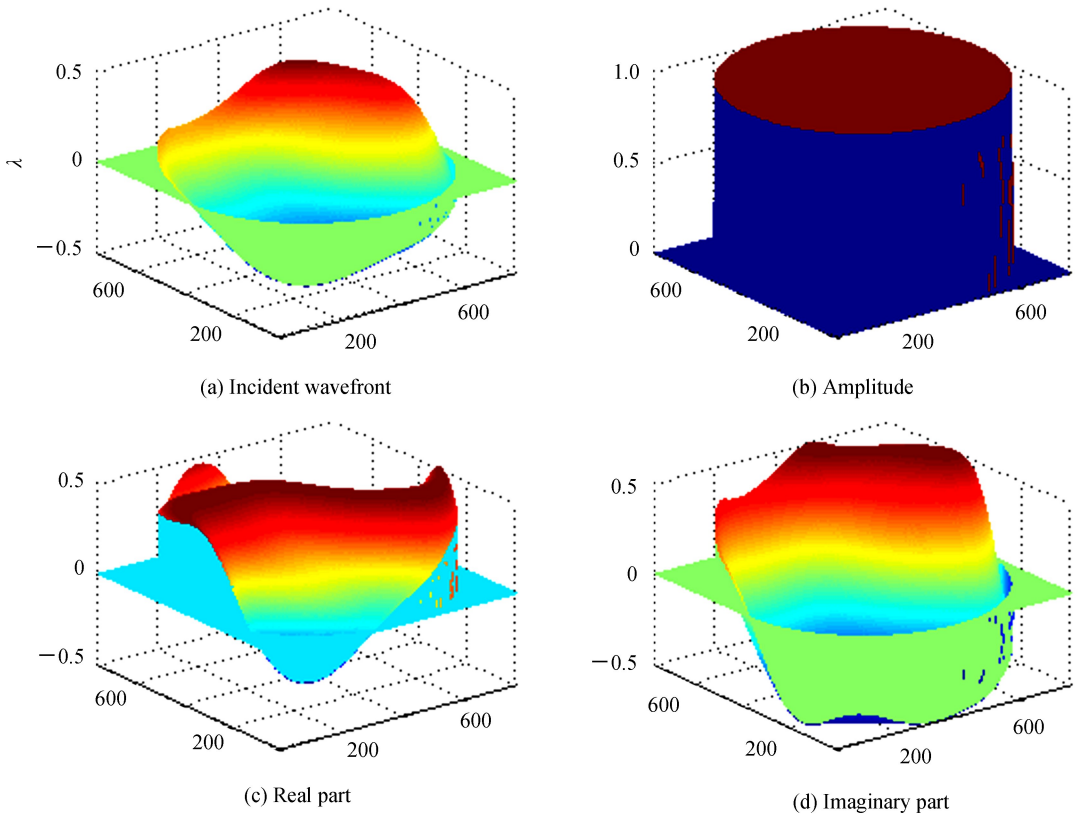

Fig.4 Incident optical field

The modulation patterns are generated from the first 256 Walsh series according to Eq. (4). These patterns are used to modulate the incident optical field. The light intensities detected with the photodiode in the focal point can be calculated based on Eq. (1). These light intensities satisfy the nonlinear Eq. (5). By solving these equations, the expansion coefficients of the real part and the absolute value of the coefficients of the imaginary part can be calculated based on Eq. (6). The real part of the optical field can be reconstructed based on Eq. (7). Fig. 5(a) shows the reconstructed real part of the optical field. Then by solving Eq. (10), the signs of the expansion coefficients of the imaginary part can be determined. Accordingly, the value of $\hat{d}$ is 0.0455. The imaginary part of the incident optical field can be reconstructed and Fig. 5(b) shows the reconstructed imaginary part. Based on Eq. (12), the incident wavefront can be reconstructed, as shown in Fig. 5(c).

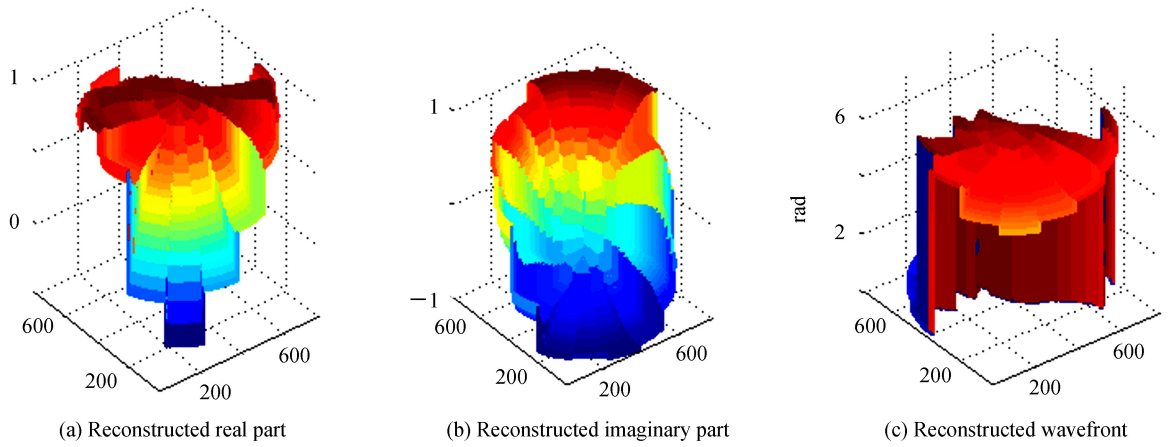

Fig.5 The reconstructed wrapped and discrete wavefront

It can be seen from Fig. 5(c) that the reconstructed discrete wavefront is a wrapped and discrete wavefront and different with the incident wavefront. In order to acquire accurate wavefront, the wrapped and discrete wavefront is unwrapped, as shown in Fig. 6(a)[17].

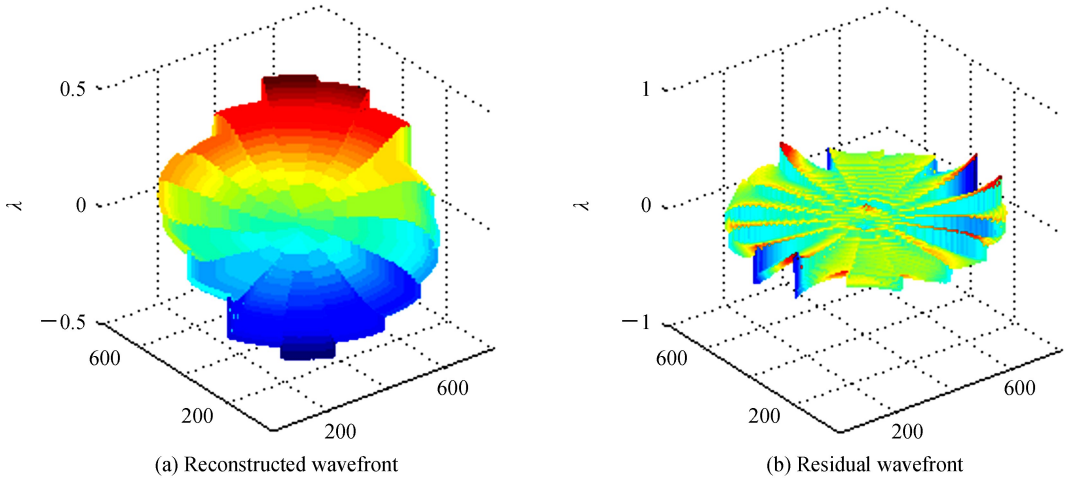

Fig.6 Unwrapped discrete wavefront

Considering the incident wavefront is continuous, it is not a good idea to describe the incident wavefront with the unwrapped discrete wavefront directly. So in order to acquire more accurate reconstructed wavefront, we do the smoothing on the discrete wavefront. Fig. 7(a) shows the smoothed wavefront and Fig. 7(b) is the residual wavefront. It can be seen from Fig. 7(b) that both PV and RMS of the residual wavefront is very small. The incident wavefront is reconstructed accurately.

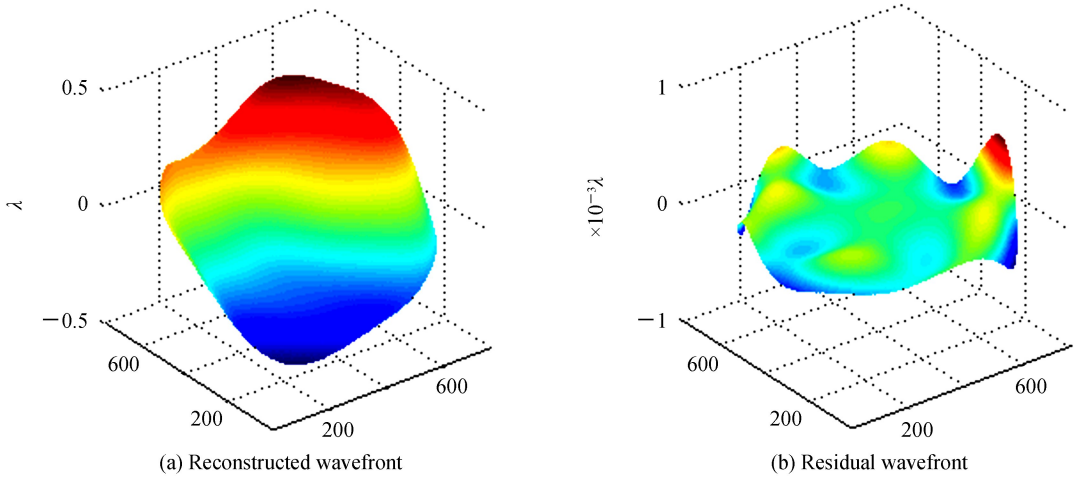

Fig.7 Reconstructed continuous wavefront

In order to validate the feasibility of the method more fully, 100 stochastic wavefront are produced and reconstructed with the method. Fig. 8 shows the wavefront reconstruction result. The vertical ordinate is the ratio of the RMS of the residual wavefront and the RMS of the stochastic wavefront. Horizontal ordinate is wavefront reconstruction time. It can be seen from that the stochastic wavefront can be reconstructed correctly.

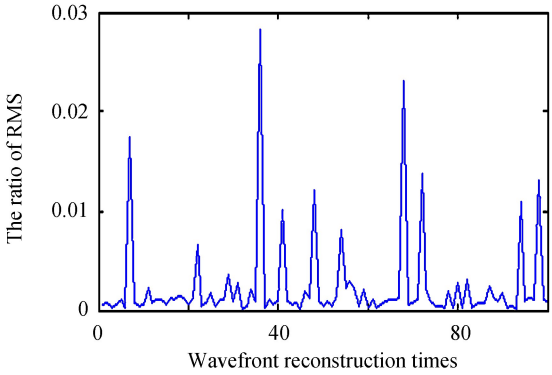

Fig.8 Theerror of wavefront reconstruction

The light intensity distribution of the incident may be not uniform. In order to research the feasibility of the method, wavefront reconstruction is simulated. Fig. 9 shows the wavefront reconstruction with uneven light intensity distribution.

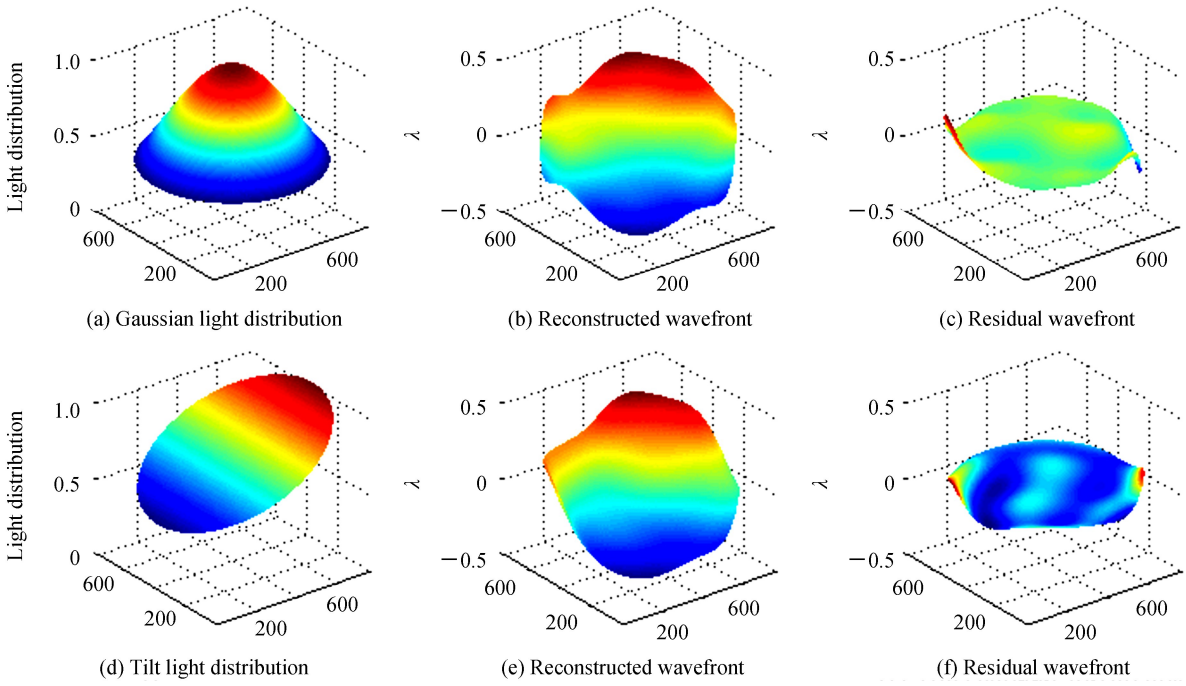

Fig.9 Wavefront reconstruction with uneven light distribution

It can be seen from Fig. 9 that the wavefront reconstruction method works well with uneven light distribution.

3 Error analysis of wavefront reconstruction

The same incident wavefront isreconstructed with the existing method described in Ref. [14], as shown in Fig. 10. Meanwhile, the value of $\hat{d}_0$ calculated based on Eq. (10) and its value is 0.045 7. The value of $\hat{d}_0$ is larger than the value acquired in the proposed method. But the existing method provides analytic solutions of the expansion coefficients of the optical field. And the simulation result shows that the wavefront reconstruction accuracy of the existing method is higner than that of the proposed method. It

means that the sign of the expansion coefficients of the imaginary part when $\hat{d}$ reaches its minimum.

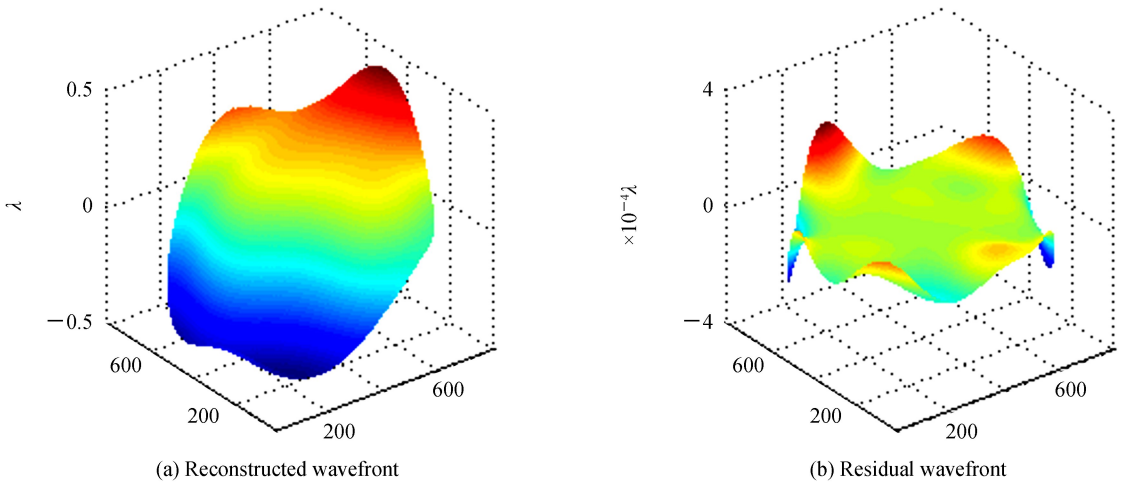

Fig.10 Reconstructed wavefront and residual wavefront (PV=0.000 41λ, RMS=0.000 033λ)

As shown in Eq. (2), the optical field is expressed with Walsh functions.It means the optical field of single segment is equal in the expression. Accordingly, the light intensity and phase is equal too. We can get that

$$\iint_{S_1} A\,\mathrm{e}^{\mathrm{i}\varphi}\,\mathrm{d}x\,\mathrm{d}y = \iint_{S_1} A_1\,\mathrm{e}^{\mathrm{i}\varphi_1}\,\mathrm{d}x\,\mathrm{d}y \tag{13}$$

where S_1 is the square of the segment. A_1 and φ_1 are the equivalent amplitude and phase. Considering the value of φ is fluctuant slightly, we can get that

$$\left|\iint_{A_1} \mathrm{e}^{\mathrm{i}\varphi}\,\mathrm{d}x\,\mathrm{d}y\right| < \left|\iint_{A_1} \mathrm{e}^{\mathrm{i}\varphi_1}\,\mathrm{d}x\,\mathrm{d}y\right| \tag{14}$$

The equivalent amplitude changes as φ fluctuates. Fig. 11 shows the equivalent light intensity distribution. It can be seen that the equivalent light intensity distribution is not equal any more.

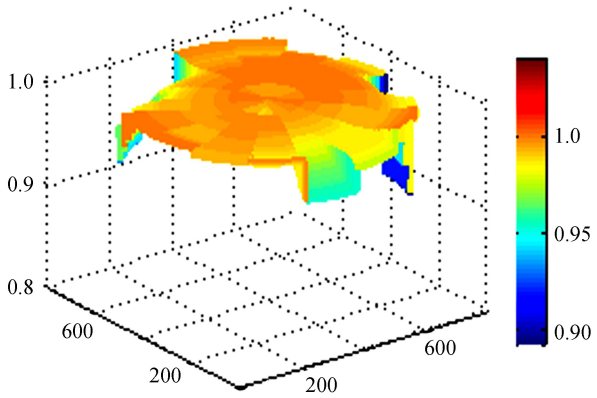

Fig.11 Equivalent light intensity distribution

We set the value of A^2 in Eq. (10) to be the light intensity distribution shown in Fig. 11 and optimize the value of $\hat{d}$. The reconstructed wavefront is shown as Fig. 12.

By comparing Fig. 12(b) with Fig. 10(b), the proposed wavefront method can acquire same wavefront reconstruction precision. It demonstrate that the wavefront reconstruction error of the proposed method is from the non uniform light intensity distribution caused by the phase fluctuating in single segment. But considering the square of each segment usually is very small, the phase fluctuating is very small in single segment accordingly. So the reconstructed wavefront acquired by the proposed method is accurate and reliable.

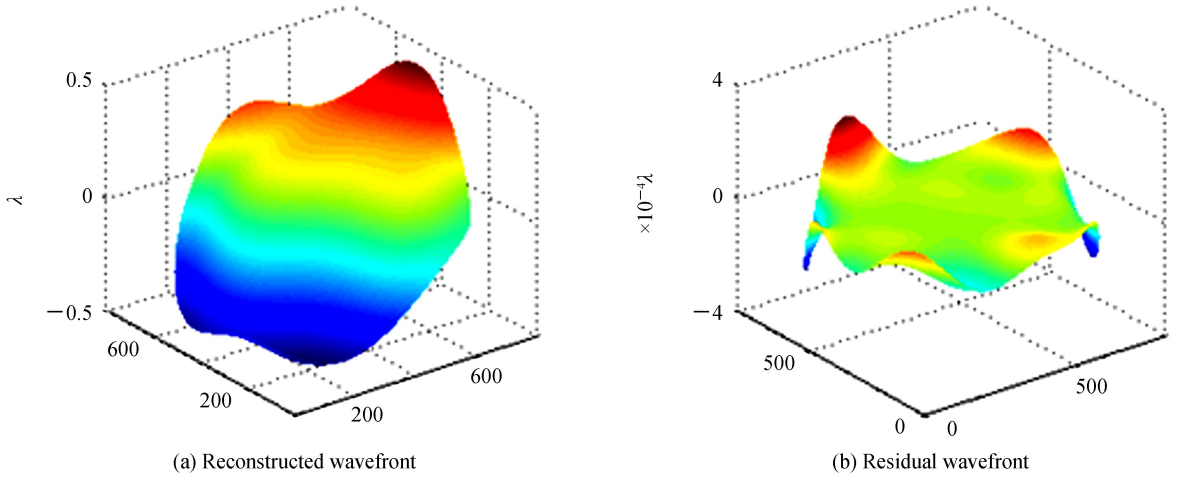

Fig.12 Wavefront reconstruction based on the equivalent light intensity distribution

4 Experiment

The experimental apparatus is shown in Fig.13. The light beam is modulated with DMD and focused with lens. Then a pinhole is placed in the focus point to filter the light and the photodiode is used to detected the light in the pinhole.

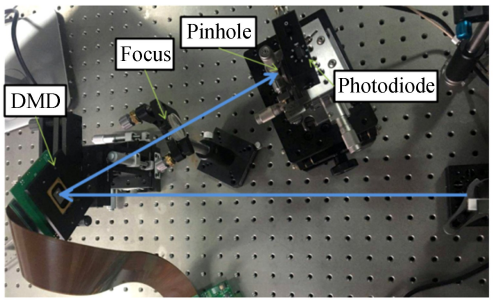

Fig.13 Experimental setup for wavefront sensing

A tilt aberration (PV=0.67λ, RMS=0.17λ) is introduced into the incident wavefront and the light intensities are detected with photodiode. Fig. 14(a) shows the reconstructed wavefront tilt aberration. It can be seen that the RMS of the residual wavefront is less than 0.2 times of the RMS of the incident wavefront. The tilt aberration is reconstructed. The feasibility of the method is validated.

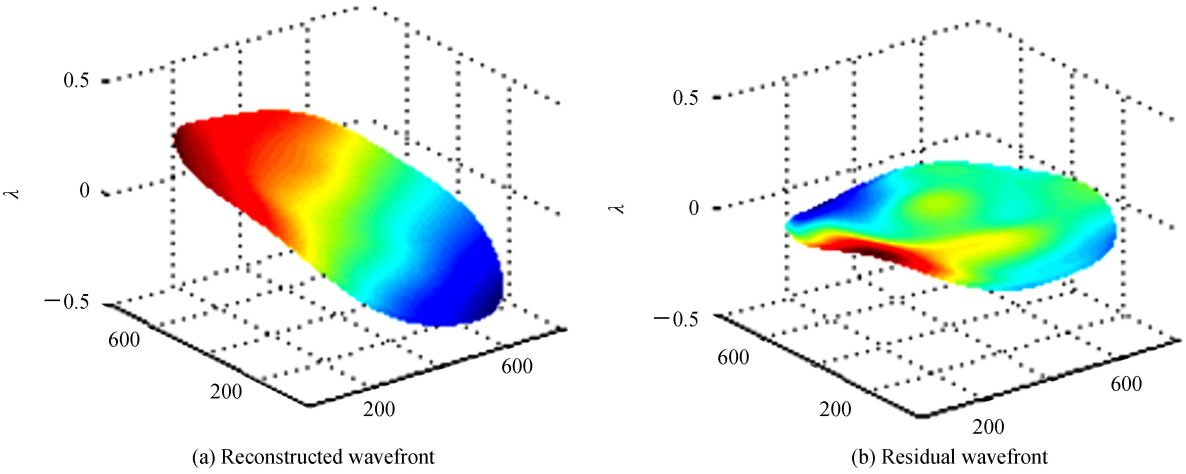

Fig.14 Tilt aberration reconstruction

5 Conclusion

A wavefront reconstruction method based on binary complementary modulation modes is proposed. The expansion coefficients of the imaginary part of the optical field are determined based on the light intensity distribution in the method. The wavefront reconstruction method realizes wavefront reconstruction precisely. And the sampling frequency of the proposed method is 1.5 times of the method described in Ref.[14]. The numerical simulations and experiments also prove the feasibility of the method.

References

[1] LIANG J, GRIMM B, GOELZ S, *et al*. Objective measurement of wave aberrations of the human eye with the use of a Hartmann-Shack wave-front sensor.[J]. *Journal of the Optical Society of America A*, 1994, **11**(7):1949.

[2] HARDY J W, THOMPSON L. Adaptive optics for astronomical telescopes[J]. *Physics Today*, 2000, **53**(4):69-69.

[3] RAO C, JIANG W, LING N. Atmospheric characterization with Shack-Hartmann wavefront sensors for non-Kolmogorov turbulence[J]. *Optical Engineering*, 2002, **41**(2):534-541.

[4] RODDIER F. Curvature sensing and compensation: a new concept in adaptive optics[J]. *Applied Optics*, 1988, **27**(7): 1223.

[5] RODDIER F J, GRAVES J E, LIMBURG E J. Seeing monitor based on wavefront curvature sensing[C]. SPIE, 1990, 1236:474-479.

[6] YANG Q, FTACLAS C, CHUNM. Wavefront correction with high-order curvature adaptive optics systems[J]. *Journal of the Optical Society of America A: Optics Image Science & Vision*, 2006, **23**(6):1375-1381.

[7] GERCHBERG R W, SAXTON W O. Phase determination for image and diffraction plane pictures in the electron microscope[J]. *Optik - International Journal for Light and Electron Optics*, 1971, **34**:275-284.

[8] GERCHBERG R W. A practical algorithm for the determination of phase from image and diffraction plane pictures[J]. *Optik*, 1972, **35**:237-250.

[9] TESCHER A G. Wavefront sensing by phase retrieval[C]. SPIE, 1982, **207**:32-39.

[10] WANG F. Wavefront sensing through measurements of binary aberration modes[J]. *Applied Optics*, 2009, **48**(15): 2865-2870.

[11] WANG S, YANG P, AOM, *et al*. Wavefront sensing by means of binary intensity modulation.[J]. *Applied Optics*, 2014, **53**(35):8342-8349.

[12] BOOTHM J. Wave front sensor-less adaptive optics: a model-based approach using sphere packings[J]. *Optics Express*, 2006, **14**(4):1339-1352.

[13] SONG H, FRAANJE R, SCHITTER G, *et al*. Model-based aberration correction in a closed-loop wavefront-sensor-less adaptive optics system[J]. *Optics Express*, 2010, **18**(23):24070-24084.

[14] PANG B, WANG S, CHENG T, *et al*. Wavefront reconstruction algorithm for wavefront sensing based on binary aberration modes[J]. *Chinese Physics B*, 2017, **26**(5):153-159.

[15] RI S, FUJIGAKI M, MATUI T. *et al*. DMD camera and its applications to fringe pattern analysis[C].Proceedings of the SEM Annual Conference and Exposition on Experimental and Applied Mechanics, 2007, **3**: 1462-1468

[16] WALSH J L. A closed set of normal orthogonal functions[J]. *American Journal of Mathematics*, 1922, **45**(1):5-24.

[17] BEAUCHAMP K G.Walsh functions and their applications[J]. *Proceedings of the IEEE*, 1975, **65**(2):285-285.

[18] SALAH K. Two-dimensional phase unwrapping[J]. *Science*, 2007, **310**(5755):1770-1771.

[19] WANG S, YANG P, DONG L, *et al*. A transformation approach for aberration-mode coefficients of Walsh functions and Zernike polynomials[C]. SPIE, 2015, **9255**:92553C

[20] NOLL R J. Zernike polynomials and atmospheric turbulence[J]. *Journal of the Optical Society of America*, 1976, **66** (3):207-211.

引用格式:PANG Bo-qing, WANG Shuai, YANG Ping. Wavefront Reconstruction Based on Binary Complementary Modulation Modes[J]. *Acta Photonica Sinica*, 2018, **47**(10):1011002

庞博清,王帅,杨平. 基于二元互补调制模式的波前重构[J].光子学报,2018,**47**(10):1011002